Direct Concentration Approach of Moisture Diffusion and Whole-Field Vapor Pressure Modeling for Reflow Process—Part I: Theory and Numerical Implementation

B. Xie
Advanced Electronic Manufacturing Center,
School of Mechanical Engineering,
Shanghai Jiao Tong University,
Shanghai 200240, China

X. J. Fan[1]
Department of Mechanical Engineering,
P.O. Box 10028,
Lamar University,
Beaumont, TX 77710;
Department of Engineering Mechanics,
South China University of Technology,
Guangzhou 510640, China
e-mail: xuejun.fan@lamar.edu

X. Q. Shi
Hong Kong Applied Science and Technology
Research Institute,
2 Science Park East Avenue,
Shatin, Hong Kong

H. Ding
Advanced Electronic Manufacturing Center,
School of Mechanical Engineering,
Shanghai Jiao Tong University,
Shanghai 200240, China

*Moisture concentration is discontinuous at interfaces when two materials, which have different saturated moisture concentrations, are joined together. In order to perform moisture diffusion modeling in a multimaterial system such as electronic packages, normalization methods have been commonly used to remove the discontinuity of moisture concentration at interfaces. However, such treatments cannot be extended to a reflow process, in which ambient temperature and/or humidity vary with time. This paper develops a direct concentration approach, with which the moisture concentration is used as a field variable directly. Constraint equations are applied to meet the interface continuity requirements. Further in this paper, a simplified vapor pressure model based on a multiscale analysis is developed. The model considers the phase change in moisture, and links the macroscopic moisture concentration to the moisture state at a microscopic level. This model yields the exact same results with the original vapor pressure model (Fan, et al., 2005, "A Micromechanics Based Vapor Pressure Model in Electronic Packages," ASME J. Electron. Packag., **127**(3), pp. 262–267). The new model does not need to relate to a reference temperature state. Numerical implementation procedures for calculating moisture concentration and ensuing vapor pressure, which are coupled with temperature analysis, are presented in this paper.* [DOI: 10.1115/1.3144147]

Keywords: direct concentration approach (DCA), moisture diffusion, vapor pressure, reflow, electronic package, multiscale analysis

1 Introduction

Moisture plays an important role in the integrity and reliability of plastic microelectronics packaging. The structural integrity of electronic packages is significantly influenced by the presence of moisture in packages. Many failures in microelectronics packages can be traced back to moisture [1–3]. When atmospheric moisture is absorbed through the packaged microelectronics devices, it condenses in free volumes or nanopores in polymer materials, and along interfaces. The condensed moisture will vaporize and produce high vapor pressure during surface mount process, in which the devices and printed circuit boards are entirely placed in a reflow oven. A reflow process is completed within a few minutes, and the peak temperature of devices during reflow typically ranges from 220°C to 260°C. Polymer materials, such as dielectric films, adhesives, encapsulants, and plastic printed circuit boards, become extremely compliant when temperature exceeds their glass transition temperatures. In addition, the interfacial adhesion strength drops substantially. As a result, delamination may occur at weak interfaces due to the combined effects of thermomechanical stresses, hygroscopic stresses, vapor pressure, material softening, and adhesion degradation. An audible sound may be produced if water vapor is suddenly released due to material cracking.

Moisture diffusion and vapor pressure analysis is a key to understanding moisture-induced failure mechanism in electronic packaging. Kitano et al. [4] and Tay and Lin [5] investigated the coupled moisture diffusion and heat transfer in plastic electronic packages. In the work of Tay and Lin [5], the normalized approach is used for a moisture diffusion analysis. Galloway and Miles [6] characterized moisture properties for different packaging materials and introduced thermal-moisture analogy methodology for moisture diffusion analysis. Wong et al. [7] introduced an alternative normalized variable, so-called "wetness," which is defined as the ratio of moisture concentration over its saturated moisture concentration. The discontinuity of moisture concentration at interfaces thus can be removed by using those normalized variables. Commercially available heat conduction software can be applied directly to solve moisture diffusion problems.

Typical moisture sensitivity/reflow test is involved with two stages, moisture absorption at a constant temperature/humidity condition (preconditioning), followed by a simulated reflow process. Moisture absorbed during preconditioning will be partially released at reflow, as the humidity in reflow oven is virtually zero. Traditional analysis usually neglects the moisture loss during reflow due to the fact that the local moisture concentration at critical interfaces inside packages remains intact [8,9]. For ultrathin small-form factor packages, however, the local moisture concentration in packages becomes very sensitive to package geometry

---

[1] Corresponding author.

Contributed by the Electrical and Electronic Packaging Division of ASME for publication in the JOURNAL OF ELECTRONIC PACKAGING. Manuscript received January 9, 2008; final manuscript received March 22, 2009; published online July 31, 2009. Assoc. Editor: Cemal Basaran.

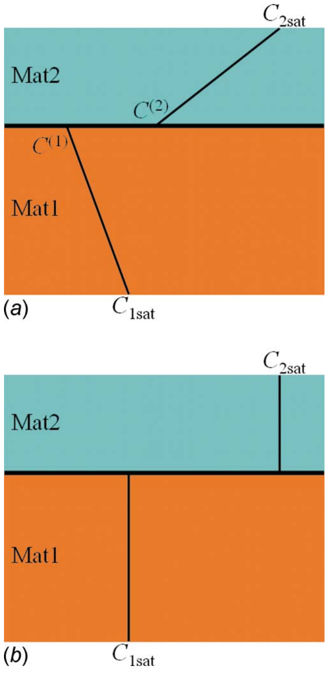

Fig. 1 Schematic of moisture distribution in bulk and at interface for a bimaterial: (*a*) unsaturated case and (*b*) saturated case

[10]. Hence it is important to understand the moisture redistribution, transport, and diffusion during the reflow process. It was found that the normalization approach cannot be applied to a loading condition with varying ambient temperature and/or humidity, such as in reflow [11]. This is because the simple thermal-moisture analogy does not exist anymore in this case. Moisture desorption analysis using normalization approach was conducted previously [8,9]. The validity is strictly limited to an assumption that the saturated moisture concentration is independent of temperature.

In this paper, a named direct concentration approach (DCA) is developed to solve moisture diffusion problems under varying ambient temperatures and humidity loading conditions. In the DCA, the moisture concentration is used as a basic field variable, which is discontinuous at interfaces. Constraint equations are applied at interfaces to satisfy the interface continuity requirement. Furthermore, this paper develops a simplified vapor pressure model, which follows the concept of a multiscale micromechanics analysis developed by one of the authors previously [8,12,13]. The free volume fraction is introduced to describe the moisture density in the interstitial spaces of porous material. Phase change in moisture is considered during temperature change. The details of numerical treatment and implementation procedures are presented. A user-defined FORTRAN subroutine is developed to visualize the whole-field vapor pressure distribution using ABAQUS™.

2 Direct Concentration Approach

2.1 Normalization Approach. Moisture concentration is discontinuous at interfaces when two materials, which have different saturated moisture concentrations (C_{sat}), are joined together. As shown in Fig. 1, for unsaturated and saturated situations, respectively, the moisture concentration at interface is given by

$$C^{(1)} \neq C^{(2)} \tag{1}$$

where $C^{(1)}$ is the moisture concentration at the interface on the material 1 (Mat1) side, and $C^{(2)}$ is the moisture concentration at the interface on the material 2 (Mat2) side.

However, the interfacial continuity can be expressed by

$$\frac{C^{(1)}}{S_1} = \frac{C^{(2)}}{S_2} \tag{2}$$

where S_1 and S_2 are the solubilities of Mat1 and Mat2, respectively. Solubility is a material property and a function of temperature only. From Eqs. (1) and (2), the interfacial discontinuity can be removed by normalizing the moisture concentration C as follows:

$$\varphi = C/S \tag{3}$$

When Fick's law is used, transient moisture diffusion is governed by a similar governing differential equation used for transient heat transfer analysis. Galloway and Miles [6] demonstrated that the commercially available finite element software for transient heat transfer analysis can be used for transient moisture diffusion modeling, as long as the field variable of temperature T in a transient thermal analysis is replaced by the field variable φ, defined in Eq. (3). Similarly, Wong et al. [7] introduced an alternative variable, so-called wetness w, which is defined as

$$w = C/C_{sat} \tag{4}$$

The wetness w is also continuous at interfaces because the saturated moisture concentration C_{sat} is related to the solubility S according to Henry's law as follows:

$$S = C_{sat}/p_{ext} \tag{5}$$

where p_{ext} is the ambient vapor pressure at the given temperature and humid condition. It is noted that C_{sat} is not strictly a material property since it depends on ambient humidity (RH).

When Fick's law is used, the transient moisture diffusion is given by

$$\frac{\partial^2 C}{\partial x^2} + \frac{\partial^2 C}{\partial y^2} + \frac{\partial^2 C}{\partial z^2} = \frac{1}{D}\frac{\partial C}{\partial t} \tag{6}$$

where x, y, and z are coordinates; D is the moisture diffusivity; and t is the time. Secondary moisture transport mechanisms are ignored in developing Eq. (6). It is found that Eq. (6) may not be used in a multimaterial system since the field variable, i.e., moisture concentration C, is discontinuous at interfaces. Normalized variables such as φ or w can be applied to remove the interfacial discontinuity. When Eq. (3) is applied, and only when the solubility S remains constant for each material during the entire time period under study, Eq. (6) can be rewritten in terms of φ as

$$\frac{\partial^2 \varphi}{\partial x^2} + \frac{\partial^2 \varphi}{\partial y^2} + \frac{\partial^2 \varphi}{\partial z^2} = \frac{1}{D}\frac{\partial \varphi}{\partial t} \tag{7a}$$

with

$$\varphi_1 = \varphi_2 \tag{7b}$$

$$\alpha_{D1} S_1 \frac{\partial \varphi_1}{\partial n} = \alpha_{D2} S_2 \frac{\partial \varphi_2}{\partial n} \tag{7c}$$

Similarly, when w is applied, Eq. (6) can be rewritten in terms of w as

$$\frac{\partial^2 w}{\partial x^2} + \frac{\partial^2 w}{\partial y^2} + \frac{\partial^2 w}{\partial z^2} = \frac{1}{D}\frac{\partial w}{\partial t} \tag{8a}$$

$$w_1 = w_2 \tag{8b}$$

$$\alpha_{D1} C_{sat1} \frac{\partial w_1}{\partial n} = \alpha_{D2} C_{sat2} \frac{\partial w_2}{\partial n} \tag{8c}$$

when the saturated moisture concentration is a constant.

It can be seen that the normalized variables φ and w are now continuous at interfaces.

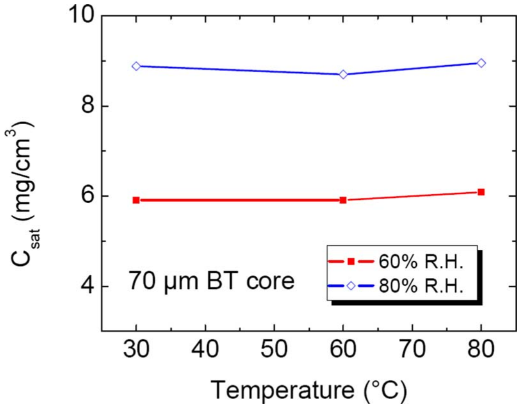

Fig. 2 Saturated moisture concentration as a function of temperature of a BT sample for two different RH levels [14]

2.2 Direct Concentration Approach. Now consider a general case in which the solubility S varies with time t. A simple transformation from Eq. (6) to Eq. (7) does not exist, but is given by

$$\frac{\partial^2\varphi}{\partial x^2}+\frac{\partial^2\varphi}{\partial y^2}+\frac{\partial^2\varphi}{\partial z^2}=\frac{1}{D}\frac{\partial\varphi}{\partial t}+\frac{\varphi}{D\cdot S}\frac{\partial S}{\partial t} \tag{9}$$

in which

$$\frac{\varphi}{D\cdot S}\frac{\partial S}{\partial t}\neq 0 \tag{10}$$

Similarly,

$$\frac{\partial^2 w}{\partial x^2}+\frac{\partial^2 w}{\partial y^2}+\frac{\partial^2 w}{\partial z^2}=\frac{1}{D}\frac{\partial w}{\partial t}+\frac{w}{D\cdot C_{sat}}\frac{\partial C_{sat}}{\partial t} \tag{11}$$

in which

$$\frac{w}{D\cdot C_{sat}}\frac{\partial C_{sat}}{\partial t}\neq 0 \tag{12}$$

when the saturated moisture concentration C_{sat} becomes dependent on time t. In Eqs. (9) and (11), S or C_{sat} is assumed coordinate-independent for simplification.

Equations (9) and (11) indicate that a simple thermal-moisture analogy does not exist when ambient temperature or humidity varies with time (or temperature). For a reflow process, the ambient humidity condition can be assumed constant (zero), but temperature changes with time. In this case, Eq. (10) holds true.

Equation (11) can be reduced to Eq. (8a) only when the saturated moisture concentration is a constant. For most polymer materials, it was found that C_{sat} is relatively independent of temperature, but RH [1]. Figure 2 is an example of the saturated moisture concentration in a bismaleimide-triazine (BT) sample as a function of temperature for two different RH levels [14]. It clearly shows that C_{sat} in BT core is essentially temperature independent. On the other hand, Fig. 3 plots the saturated moisture concentration for a low-Tg die-attach film as a function of temperature at 60%RH level [15]. It shows a strong dependency with temperature. This film has Tg around 35°C. It reveals that the saturated moisture concentration depends strongly on temperature across its glass transition temperature. Most polymer materials in electronic packages have a glass transition temperature lower than the peak reflow temperature. It becomes evident that the saturated moisture concentration is not a constant during reflow.

A DCA is introduced to correctly perform the moisture diffusion modeling under varying temperatures and humidity conditions. In the DCA, the moisture concentration C is directly used as the basic field variable. Therefore, the governing differential equation is given by

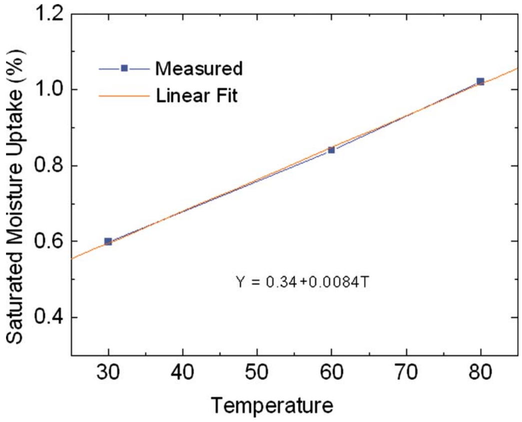

Fig. 3 Saturated moisture concentration as a function of temperature for a low-Tg die-attach film at 60%RH level [15]

$$\frac{\partial^2 C}{\partial x^2}+\frac{\partial^2 C}{\partial y^2}+\frac{\partial^2 C}{\partial z^2}=\frac{1}{D(t)}\frac{\partial C}{\partial t} \tag{13}$$

It should be noted that the diffusivity D is a function of time (or temperature), and C is discontinuous at interfaces. Additional treatment is necessary to ensure the following continuous conditions at interfaces:

$$\frac{C^{(1)}}{S(t)^1}=\frac{C^{(2)}}{S(t)^2} \tag{14}$$

$$D_1(t)\frac{\partial C^{(1)}}{\partial n}=D_2(t)\frac{\partial C^{(2)}}{\partial n} \tag{15}$$

where $D_1(t)$ and $D_2(t)$ are the moisture diffusivities of Mat1 and Mat2, respectively, and n is the normal direction of the location at interfaces.

In order to satisfy the interfacial continuity conditions, two separate sets of nodes are applied at a bimaterial interface to represent the discontinuity of the moisture concentration, as shown in Fig. 4. A constraint equation is applied for each pair of nodes based on the Eq. (14) to join two materials together. The constraint equation is given by

$$C^{(1)}/C^{(2)}=S_1(t)/S_2(t) \tag{16}$$

According to the variational principle, Eq. (15) will be automatically satisfied through the finite element formulation as long as Eq. (16) is guaranteed.

3 Whole-Field Vapor Pressure Model

Although moisture diffusion is analyzed at a macroscopic level, the vapor pressure model should be considered at a microscopic level since moisture exists anywhere in polymer materials, and stays either in the mixed liquid/vapor phase or single vapor phase in nanopores or free volumes. Moisture is absorbed into polymeric materials in two ways. The first is as free or "unbound" water liquid or vapor, which collects at micro-/nanopores, free volumes, interfaces, and/or micro-/macrovoids. Majority of the absorbed moisture stays in unbound water state [15]. Moisture can also be

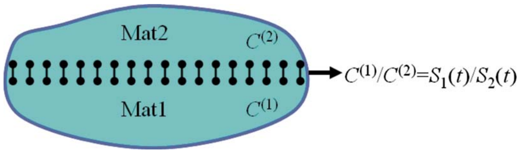

Fig. 4 Special treatment and constrain equations at a bimaterial interface in the DCA

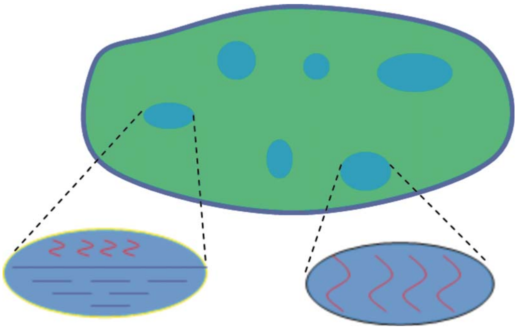

Fig. 5 Two distinct states of moisture in pores in polymer materials

absorbed by water-polymer affinity due to the availability of hydrogen bonding sites along the polymer chains and interfaces, which are known as "bound water." Unbound moisture will vaporize during reflow. In order to determine the vapor pressure, it is necessary to determine if moisture is in vapor phase or binary liquid/vapor phase. Therefore, a representative elementary volume (REV) around any considered point in porous medium is introduced. The REV is defined in such a way that wherever it is placed within the considered porous medium domain, it always contains both the solid polymer phase and porous/free volume phase. The total moisture content in a REV is obtained from the local moisture concentration C at a macroscopic level. If the free volume fraction f is known, the "apparent" moisture density ρ in pores can be defined as [13]

$$\rho = \frac{M_{\mathrm{H_2O}}}{V_f} = \frac{CV}{V_f} = \frac{C}{f} \tag{17}$$

where $M_{\mathrm{H_2O}}$ is moisture mass in free volume within a REV, V is the volume of REV, V_f is the free volume, $f = V_f/V$ and C is the moisture concentration at the location of interest.

When the moisture density ρ in pores is less than the saturated water vapor density ρ_g, the moisture is in the single vapor phase. In this case, since the total moisture content and the free volume are known, the vapor pressure can be obtained using the ideal gas law as follows:

$$p(T) = \frac{M'_{\mathrm{H_2O}}RT}{V_f} = \frac{CVRT}{MM_{\mathrm{H_2O}}V_f} = \frac{CRT}{MM_{\mathrm{H_2O}}f}$$

when

$$C(T)/f < \rho_g(T) \tag{18}$$

$M'_{\mathrm{H_2O}}$ is moisture mass in mol, and where R is the universal gas constant (=8.314 J/(mol K)), $MM_{\mathrm{H_2O}}$ is the molecular mass of water (=18 g/mol) per mol.

On the other hand, when the moisture density ρ is equal or greater than the saturated water vapor density ρ_g, the moisture in pores is in the mixed liquid-vapor phase. Therefore the vapor pressure remains as the saturated vapor pressure, as follows:

$$p(T) = p_g(T)$$

when

$$C(T)/f \geq \rho_g(T) \tag{19}$$

where p_g is the saturated water vapor pressure, which increases exponentially with temperature, as shown in the Appendix.

Figure 5 illustrates the two distinct moisture states in pores. As shown in Fig. 5, these two cases will fully describe the moisture states in pores. The above analysis has greatly simplified the original vapor pressure model [13], in which three distinct cases are identified to describe the moisture states in pores. The newly developed model does not need to relate the current moisture state to a reference moisture state, but yields the exact same results with the original model.

One of critical parameters in the above vapor pressure model is the free volume fraction f. An approximate estimation method to obtain the free volume fraction of polymers was proposed using moisture weight gain test [12,15]. Since the density of the liquid water is 1.0 g/cm^3, the moisture density in free volume, according to Eq. (17), must be less than or equal to 1.0 g/cm^3.

$$f_0 \geq C_{\mathrm{sat}} \tag{20}$$

when C_{sat} uses the unit of g/cm^3. In general, C_{sat} depends on the relative humidity and temperature. If water fills the free volume completely at 100%RH, the free volume fraction can be estimated from Eq. (20). An initial free volume fraction can be estimated from a moisture weight gain test using C_{sat} measurement data and then extrapolated to the 100%RH condition. The results based on Eq. (20) using the material property data measured by Galloway and Miles [6] showed that the free volume fraction is usually between 1% and 5% among different packaging materials.

4 Numerical Implementation

Because the material solubility is a function of temperature (thus time), the interfacial constraint equations by Eq. (16) change with time. Commercially available finite element software such as ABAQUS does not allow automatic updating of the constraint equations during analysis. In order to update the interfacial continuous conditions, a new "job" must be defined and executed with the updated moisture distribution of previous time step as the initial moisture distribution for the next step analysis. Failure in updating constraint equations will result in wrong results.

A simple transformation from moisture diffusion to a whole-field vapor pressure analysis can be done through the vapor pressure model developed in Sec. 3 as long as the free volume fraction f is known. A user-defined FORTRAN subroutine is written for ABAQUS to compute the values of vapor pressure and display the contour of vapor pressure at each step. The contours of both moisture distribution and vapor pressure can therefore be graphically visualized.

As studied by Tay and Lin [5], the temperature and moisture fields are sequentially-coupled during the reflow process. Temperature distribution will affect the moisture diffusion since the diffusivity and solubility are the functions of temperature. It has been shown previously that the heat transfer process is a few orders faster than moisture diffusion, thus the problem may be uncoupled [1]. For ultrathin packages, however, the coupling effect must be considered. When ABAQUS is used, the "MASS DIFFUSION" analysis type is applied for moisture diffusion. The temperature field is obtained from the "HEAT TRANSFER" analysis type. All material properties can be considered as functions of temperatures. Since the constraint equations at interfaces need to be updated at each incremental temperature step, a special program is written to allow continuous calculations for an entire reflow process. The general implementation procedures of the moisture diffusion and vapor pressure modeling are summarized in Fig. 6.

5 Verification

A simple bimaterial problem is analyzed, as shown in Fig. 7(*a*) (Mat1 represents material 1 and Mat2 represents material 2, respectively), to verify the DCA and the implementation procedure. Figure 7(*a*) is a two-step loading problem. Step 1 is moisture absorption at 60°C/60%RH (for 88 h to guarantee that the materials are fully saturated). In step 2, the ambient condition experiences a step change from 60°C/60%RH to 260°C/0%RH for desorption. This two-step loading problem cannot be solved using traditional normalization methods since the ambient condition experiences a time-dependent change. The problem is now solved

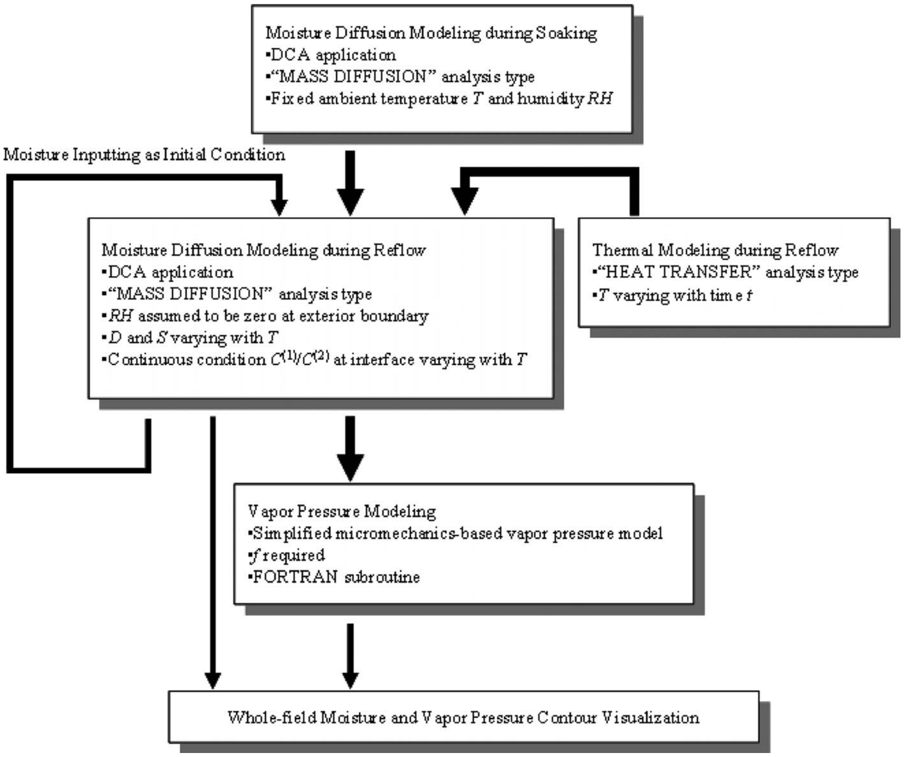

Fig. 6 Implementation procedures of sequentially-coupled heat transfer/moisture diffusion and vapor pressure modeling for reflow process

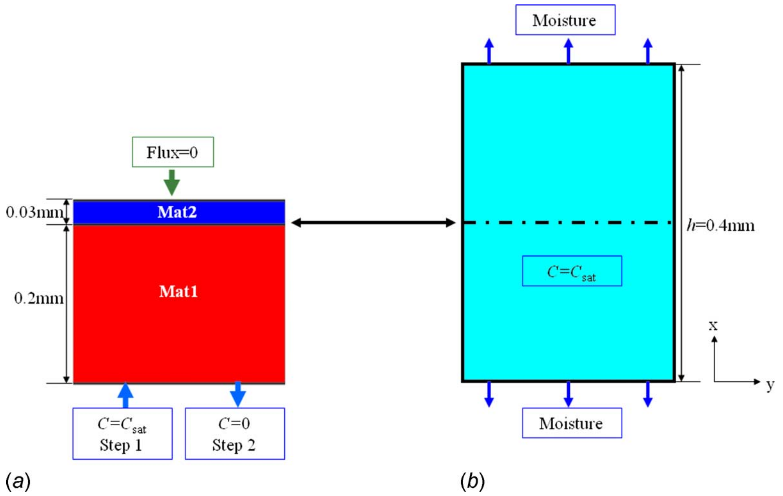

Fig. 7 (*a*) a bimaterial two-step loading problem and (*b*) a single-material problem

using the DCA according to the procedures described above. It is noted that the constraint equations at the interface from steps 1 to 2 must be updated accordingly.

In order to validate the numerical results, Mat2 is considered as a nonabsorbing material. This is realized by assigning the material properties of Mat2 a few orders lower than Mat1, as shown in Tables 1 and 2, respectively. Therefore, the problem in Fig. 7(*a*) is equivalent to a single-material problem in Fig. 7(*b*). Furthermore, only the results in step 2 are compared. In this case, the problem in Fig. 7(*b*) can be assumed as a desorption process with initially

Table 1 Material properties at 60°C/60%RH

	60°C/60%RH	
	Mat1	Mat2
Diffusivity $D(\mathrm{mm}^2/\mathrm{s})$	5.14×10^{-7}	5.14×10^{-10}
$C_{\mathrm{sat}}(\mathrm{kg/m}^3)$	4.704	4.704×10^{-3}
Solubility $S(\mathrm{kg/m}^3\ \mathrm{Pa})$	3.92×10^{-4}	3.92×10^{-7}

Table 2 Material properties at 260°C/60%RH

	260°C/60%RH	
	Mat1	Mat2
Diffusivity $D(\mathrm{mm}^2/\mathrm{s})$	5×10^{-4}	2.5×10^{-7}
$C_{\mathrm{sat}}(\mathrm{kg/m}^3)$	2.352	1.176×10^{-3}
Solubility $S(\mathrm{kg/m}^3\ \mathrm{Pa})$	8.37×10^{-7}	4.185×10^{-10}

Table 3 Saturated water vapor density and vapor pressure at different temperatures

	T (°C)																				
	60	70	80	90	100	110	120	130	140	150	160	170	180	190	200	210	220	230	240	250	260
$\rho_g(\mathrm{kg/m^3})$	0.13	0.2	0.29	0.42	0.6	0.83	1.12	1.5	1.97	2.55	3.26	4.12	5.16	6.4	7.86	9.59	11.62	14	16.76	19.99	23.73
$p_g(\mathrm{MPa})$	0.02	0.03	0.05	0.07	0.1	0.15	0.2	0.28	0.38	0.5	0.65	0.84	1.1	1.37	1.72	2.14	2.65	3.25	3.97	4.83	5.84

fully saturated condition. The analytical solution for the problem in Fig. 7(b) can be derived as follows [16]:

$$C(x,t)=\frac{4C_{\mathrm{sat}}}{\pi}\sum_{n=0}^{\infty}\frac{1}{(2n+1)}\sin\frac{(2n+1)\pi x}{h}\exp\left[-\frac{Dt}{h^2}(2n+1)^2\pi^2\right] \tag{21}$$

where C_{sat} is the saturated moisture concentration of Mat1 at 60°C/60%RH, D is the moisture diffusivity at 260°C, h is the double-thickness of Mat1 (as 0.4 mm shown in the Fig. 7(b)), and x is the distance from the edge. In this example, the saturated moisture concentration at 60°C/60%RH is the same as 260°C/60%RH. In order to eliminate the temperature gradient effect, the thermal conductivity is chosen a few orders higher than the moisture diffusivity at 260°C, so that the temperature becomes rapidly uniform in a very short time period.

Figure 8 plots the comparison of the local moisture concentration at the interface as a function of time using the DCA and the analytical solution, respectively. It shows the excellent agreement between the two solutions. This confirms that the implementation procedure is correct and the DCA is able to examine the moisture diffusion modeling under varying ambient temperatures and humidity conditions. It is also observed that the desorption process is very fast and completed in less than 200 s for the given geometry. In step 1, it needs about 80 h to reach a saturated state at 60°C/60%RH. This is because the diffusivity at 260°C is a few orders higher than that at 60°C, as shown in Tables 1 and 2.

6 Summary

Understanding of moisture absorption, desorption, and diffusion, and the ensuing vapor pressure evolution is the key to solve the problems of moisture-induced failures in electronic packages. This paper presents a DCA to perform moisture diffusion analysis for the reflow process. The commonly used thermal-moisture analogy does not exist when ambient temperature and/or humidity vary with time. In the DCA, the moisture concentration is used as a field variable directly, and the interface continuity requirement is satisfied by using constraint equations.

Moisture diffusion is a process of moisture condensation into micro-/nanopores or free volumes in polymers. Moisture diffusion is analyzed at a macroscopic level, but the vapor pressure model should be considered at a microscopic level since the moisture stays either in the mixed liquid/vapor phase or single vapor phase in micro-/nanopores or free volumes. This paper presents a vapor pressure model based on a multiscale micromechanic analysis. The free volume fraction f is introduced to link a macroscopic moisture diffusion analysis to the microscopic vapor pressure model. The phase change in moisture is considered. An approximate estimate method to obtain the free volume fraction of polymers using moisture weight gain test is introduced.

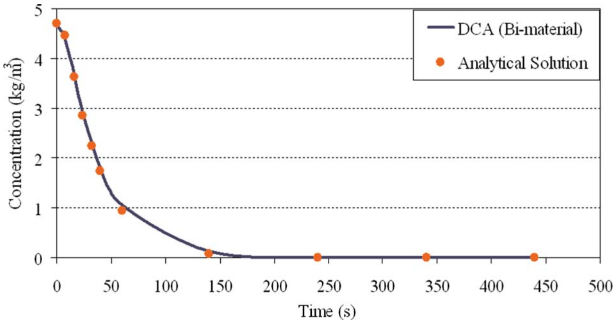

Fig. 8 Comparison of moisture concentration between the DCA and analytical solution

The numerical implementation procedures for calculating moisture concentration and ensuing vapor pressure, which are coupled with temperature analysis, are presented in this paper. It is noted that a special treatment must be made to allow the updating of the constraint equations during each incremental step. A bimaterial moisture absorption and desorption problem is solved, and the excellent agreement is obtained with an analytical solution. In Part II of this work in a separate paper, the theories and numerical implementation procedures will be applied to a 3D ultrathin stacked-die chip scale package to investigate the moisture sensitivity to substrate thickness and reflow profiles.

Appendix

Table 3 shows the saturated water vapor density and vapor pressure at different temperatures.

References

[1] Fan, X. J., 2005/2006/2007/2008, "Moisture Related Reliability in Electronic Packaging," ECTC Professional Development Course Notes.

[2] Zhang, G. Q., van Driel, W. D., and Fan, X. J., 2006, *Mechanics of Microelectronics*, Springer, New York.

[3] Fan, X. J., Zhou, J., and Chandra, A., 2008, "Package Structural Integrity Analysis Considering Moisture," Proceedings of the Electronics Components And Technology Conference, ECTC, pp. 1054–1066.

[4] Kitano, M., Nishimura, A., and Kawai, S., 1988, "Analysis of Package Cracking During Reflow Soldering Process," Proceedings of the IRPS, pp. 90–95.

[5] Tay, A. A. O., and Lin, T. Y., 1996, "Moisture Diffusion and Heat Transfer in Plastic IC Packages," IEEE Trans. Compon., Packag. Manuf. Technol., Part A, **19**(2), pp. 186–193.

[6] Galloway, J. E., and Miles, B. M., 1997, "Moisture Absorption and Desorption Predictions for Plastic Ball Grid Array Packages," IEEE Trans. Compon., Packag. Manuf. Technol., Part A, **20**(3), pp. 274–279.

[7] Wong, E. H., Teo, Y. C., and Lim, T. B., 1998, "Moisture Diffusion and Vapor Pressure Modeling of IC Packaging," Proceedings of the 48th Electronic Components and Technology Conference, pp. 1372–1378.

[8] Tee, T. Y., Fan, X. J., and Lim, T. B., 1999, "Modeling of Whole Field Vapor Pressure During Reflow for Flip Chip and Wire-Bond PGBA Packages," First International Workshop on Electronic Materials & Packaging.

[9] Tee, T. Y., and Zhong, Z. W., 2004, "Integrated Vapor Pressure, Hygroswelling and Thermo-Mechanical Stress Modeling of QFN Package During Reflow With Interfacial Fracture Mechanics Analysis," Microelectron. Reliab., **44**(1), pp. 105–114.

[10] Xie, B., Shi, X. Q., and Fan, X. J., 2007, "Sensitivity Investigation of Substrate Thickness and Reflow Profile on Wafer Level Film Failures in 3D Chip Scale Packages by Finite Element Modeling," Proceedings of the 57th Electronic Components and Technology Conference 2007, ECTC '07, pp. 242–248.

[11] Fan, X. J., Zhang, G. Q., van Driel, W. D., and Ernst, L. J., 2008, "Interfacial Delamination Mechanisms During Soldering Reflow With Moisture Preconditioning," IEEE Trans. Compon. Packag. Technol., **31**(2), pp. 252–259.

[12] Fan, X. J., and Lim, T. B., 1999, "Mechanism Analysis for Moisture-Induced Failures in IC Packages," ASME 1999 International Mechanical Engineering Congress, Paper No. IMECE/EPE-14.

[13] Fan, X. J., Zhou, J., Zhang, G. Q., and Ernst, L. J., 2005, "A Micromechanics Based Vapor Pressure Model in Electronic Packages," ASME J. Electron.

Packag., **127**(3), pp. 262–267.
[14] He, Y., and Fan, X. J., 2007, "In-Situ Characterization of Moisture Absorption and Desorption in a Thin BT Core Substrate," Proceedings of the Electronic Components and Technology Conference, pp. 1375–1383.
[15] Fan, X. J., Lee, S. W. R., and Han, Q., 2009, "Experimental Investigations and Model Study of Moisture Behaviors in Polymer Materials," Microelectron. Reliab., in press.
[16] Zhou, J., and Law, J. S.2008, "Effect of Non-Uniform Moisture Distribution on the Hygroscopic Swelling Coefficient," IEEE Trans. Compon. Packag. Technol., **31**(2), pp. 269–276.